Journal of Statistical Mechanics: Theory and Experiment
An IOP and SISSA journal

Domain walls and chaos in the disordered SOS model

K Schwarz[1], A Karrenbauer[2,3], G Schehr[4] and H Rieger[1,4]

[1] Theoretische Physik, Universität des Saarlandes, 66041 Saarbrücken, Germany
[2] Max Planck Institut f. Informatik, Universität des Saarlandes, 66041 Saarbrücken, Germany
[3] École Polytechnique Fédérale de Lausanne, 1015 Lausanne, Switzerland
[4] Laboratoire de Physique Théorique, Université de Paris-Sud, 91405 Orsay, France
E-mail: karstenschwarz@hotmail.de, andreas.karrenbauer@epfl.ch, gregory.schehr@th.u-psud.fr and h.rieger@mx.uni-saarland.de

Received 29 May 2009
Accepted 30 July 2009
Published 25 August 2009

Online at stacks.iop.org/JSTAT/2009/P08022
doi:10.1088/1742-5468/2009/08/P08022

Abstract. Domain walls, optimal droplets and disorder chaos at zero temperature are studied numerically for the solid-on-solid model on a random substrate. It is shown that the ensemble of random curves represented by the domain walls obeys Schramm's left passage formula with $\kappa = 4$ whereas their fractal dimension is $d_s = 1.25$, and therefore their behavior *cannot* be described as showing 'Schramm– (or stochastic) Loewner evolution' (SLE). Optimal droplets with a lateral size between L and $2L$ have the same fractal dimension as domain walls but an energy that saturates at a value of order $\mathcal{O}(1)$ for $L \to \infty$ such that arbitrarily large excitations exist which cost only a small amount of energy. Finally it is demonstrated that the sensitivity of the ground state to small changes of order δ in the disorder is subtle: beyond a crossover length scale $L_\delta \sim \delta^{-1}$ the correlations of the perturbed ground state with the unperturbed ground state, rescaled using the roughness, are suppressed and approach zero logarithmically.

Keywords: interfaces in random media (theory), disordered systems (theory)

ArXiv ePrint: 0905.4816

Contents

1. Introduction

Domain walls in disordered systems play an important role in understanding the stability of the ordered phase, the energetics of large scale excitations, the asymptotic dynamics in and out of equilibrium as well as the sensitivity to changes of external parameters. They have been studied quite intensively in recent years for Ising spin glasses [1]–[8], XY spin glasses [9], random field systems [10]–[13], random ferromagnets [10], disordered elastic manifolds [15]–[20], and many other systems.

Two domain wall properties are prominent. The first concerns energy and can be characterized by the behavior of the scaling of the domain wall energy with the lateral size, which gives rise to a first, sometimes universal, exponent, the stiffness exponent θ. The second concerns the geometry and gives rise to another, sometimes universal, exponent, the fractal dimension d_s, or, if the domain is not fractal, a roughness exponent ζ. The interplay between the energetics and geometry of the domain walls (i.e. between the stiffness exponent and fractal dimension) determines how sensitive the system state is to changes of either external parameters, like the temperature or a field, or internal parameters, like small disorder variations. This sensitivity is often extreme in glassy systems and goes under the name of 'chaos' [1].

Domain walls of glassy systems in two space dimensions represent fractal curves in the plane and the question arises of whether they fall into the general classification scheme for ensembles of random curves described as the Schramm– (or stochastic) Loewner evolution (SLE) scheme [21, 22]. Recently indications were found that domain walls in 2D spin glasses (at zero temperature) can indeed be described as showing SLE [23, 24], at least for a Gaussian distribution of the bonds, but apparently not for binary couplings [25]. Also the domain wall behaviors in the random bond Potts model at the critical point (i.e. at finite temperature) were found to be numerically consistent with SLE [26]. It appears natural to ask whether the domain walls in other two-dimensional disordered systems are potential candidates for a description in terms of SLE.

J. Stat. Mech. (2009) P08022

In this paper we study domain walls and chaos at zero temperature in the solid-on-solid (SOS) model on a disordered substrate. This is a numerically convenient representation of a two-dimensional elastic medium, with scalar displacement field, interacting with quenched periodic disorder. It has been studied in order to describe various physical situations ranging from vortex lattices in superconductors to incommensurate charge density waves and crystal growth on a disordered substrate [27]–[29]. Here we focus on three questions. (1) Can domain walls in this model be described as showing SLE? (2) What is the relation between the size and energy of optimal excitations (droplets) in this model? (3) Does disorder chaos exist in the ground state of this model? After a brief summary of what is already known about the model and a description of the numerical method by means of which we compute the ground state and the domain walls, these three issues are studied in separate sections. The paper ends with a discussion of the results obtained.

1.1. The model

We consider the solid-on-solid model on a disordered substrate defined by the Hamiltonian

$$H = \sum_{(ij)} (h_i - h_j)^2, \qquad h_i = n_i + d_i, \tag{1}$$

with $i \equiv (x_i, y_i) \in \mathbb{Z}^2$. In equation (1) the height variables n_i ($i = 1, \ldots, N$) take on integer values $n_i = 0, \pm 1, \pm 2, \ldots$ and the offsets d_i are independent quenched random variables uniformly distributed between 0 and 1. The sum is over all nearest neighbor pairs (ij) of a rectangular lattice of size $L_x \times L_y$ ($L_x = L_y = L$ if not stated otherwise). The boundary conditions will be specified below in the context of domain walls. The Hamiltonian in equation (1) provides a discrete model of a two-dimensional elastic medium in a disordered environment. In the continuum limit, it is described using a sine–Gordon model with random phase shifts (and in the absence of vortices), the so called Cardy–Ostlund model [30],

$$H_{\mathrm{CO}} = \int \mathrm{d}^2\mathbf{r}\, (\nabla u(\mathbf{r}))^2 - \lambda \cos(2\pi[u(\mathbf{r}) - d(\mathbf{r})]), \tag{2}$$

with a continuous scalar displacement field $u(\mathbf{r}) \in (-\infty, +\infty)$ and quenched random variables $d(\mathbf{r}) \in [0, 1]$. Discretizing the integral and taking the infinite strong coupling limit $\lambda \to \infty$ one recovers (1).

It is well known that this model, (1) and (2), displays a transition between a high-temperature phase $T > T_{\mathrm{g}} = 2/\pi$, where the disorder is irrelevant, and a low-temperature phase below T_{g}, dominated by the disorder. The high-temperature phase $T > T_{\mathrm{g}}$ is characterized by a logarithmic thermal roughness

$$C(r) = \overline{\langle (h_i - h_{i+r})^2 \rangle} \sim T \log r, \tag{3}$$

where $\langle \cdots \rangle$ denotes the thermal average and $\overline{\cdots}$ the average over the quenched disorder. The low-temperature or glassy phase is instead 'superrough', characterized by an asymptotically stronger (log-square) increase of $C(r)$:

$$C(r) \sim c(T) \log^2 r + \mathcal{O}(\log(r)), \tag{4}$$

which means $\zeta = 0$, as expected for a random periodic system. Close to T_g, a Coulomb gas renormalization group (RG) analysis to lowest order gives $c(T) \simeq (1-T/T_g)^2/2\pi^2$ [29], in rather good agreement with numerical simulations [31]. At $T = 0$, numerical simulations give the estimate $c(T = 0) \approx 0.5/(2\pi)^2 \approx 0.012$ [16, 32]. While earlier studies, based on 'nearly conformal' field theory [33], claimed an exact result for $c(T)$, predicting $c(T = 0) = 0$, in clear contradiction with the numerics, a more recent approach based on the FRG, incorporating non-analytic operators, predicts a non-zero $c(T = 0)$ which compares reasonably well with the numerics [34].

For free or periodic boundary conditions, the Hamiltonians (1) and (2) have a discrete symmetry; the energy is invariant under a global height (displacement) shift $n_i \to n_i + \Delta n$ ($u(\mathbf{r}) \to u(\mathbf{r}) + \Delta n$), where Δn is an arbitrary integer. This symmetry will not be broken in the low-temperature phase of the infinite system and true long range order at $T < T_g$ is absent, i.e. $\overline{\langle h_i \rangle} = 0$. Concomitantly the model (1), with free or periodic boundary conditions, has infinitely many ground states, which differ by a global shift $\Delta n \in \{\pm 1, \pm 2, \ldots\}$.

1.2. Domain walls

By an appropriate choice of boundary conditions one can force a domain wall into the system, which is most easily visualized at $T = 0$ (cf figure 1): consider the square geometry and fix the values of the boundary variables to $n_i = 0$. This yields a unique ground state configuration n_i^0. If one fixed the boundary variables as $n_i = +1$, the corresponding ground state would be $n'^0_i = n_i^0 + 1$. A domain wall inducing boundary condition is one in which the lower half of the boundary values are fixed at $n_i = 0$ and the upper half to $n_i^0 = 1$. The ground state of this set-up is then $\tilde{n}_i^0 = n_i^0$ in some, mainly the lower, region of the system, and $\tilde{n}_i^0 = n'^0_i$ in the rest—the two regions separated by a domain wall of non-trivial shape (see figure 1). For a continuous distribution of offsets d_i this zero-temperature domain wall is unique with probability 1, since for arbitrarily fixed boundary conditions the ground state of (1) is unique. Note that the domain wall is a single connected path from the center of the left boundary to the center of the right boundary, and cycles disconnected from this path (isolated bubbles or droplets) cannot occur in a ground state configuration since they are equivalent to excitation clusters (see below) and thus energetically unfavorable.

It turns out that these domain walls are fractal [16, 18], which means that their lengths l_{dw} scale with linear system size as

$$l_{\mathrm{path}} \sim L^{d_s}, \tag{5}$$

with $d_s > d - 1 = 1$. The numerical estimate for d_s is $d_s = 1.27 \pm 0.02$ [18]. Such a fractal scaling of zero-T domain walls is also found for spin glasses; in the 2D EA model with Gaussian couplings it is $d_{s,\mathrm{SG}} = 1.27 \pm 0.01$, and with binary couplings it is $d_{s,\mathrm{SGB}} = 1.33 \pm 0.01$. On the other hand, zero-T domain walls in disordered Ising or Potts ferromagnets are rough (i.e. are characterized by algebraic correlations) but not fractal.

The energy for such a domain wall, given by the difference between the energy of the ground state of the system with the domain wall inducing boundary conditions and the one with homogeneous boundary conditions, increases with L logarithmically:

$$\Delta E \sim \log L. \tag{6}$$

J. Stat. Mech. (2009) P08022

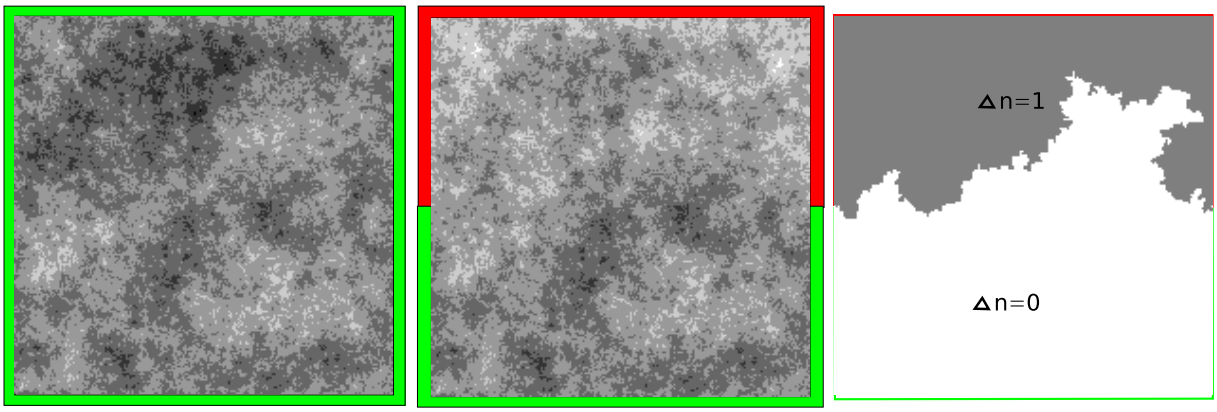

Figure 1. Left: ground state $\mathbf{n}^0$ of a 200×200 system with the boundary sites (indicated in green) fixed at $n_i = 0$. The different height values n_i are gray-coded (dark = low values, bright = high values). Middle: ground state configuration of the same system as to the left with the upper half of the boundary sites (indicated in red) fixed at $n_i = 1$ and the lower half (indicated in green) at $n_i = 0$. Right: plot of the difference between the left and middle plots: in the lower white region the ground state configuration is identical to the corresponding sites in the left figure, whereas in the upper gray region they differ by exactly $\Delta n = 1$ from the corresponding site in the middle panel. The border between the white and the gray regions is a domain wall, representing a step in the height profile of the ground state.

This result, which was obtained by numerical simulations [16], is consistent with the usual scaling relation $\Delta E \sim L^{\theta}$ together with the exact result $\theta = d - 2 + 2\zeta = 0$ (thanks to statistical tilt symmetry [35]). This logarithmic behavior is characteristic of a *marginal* glass phase, described as a line of fixed points indexed by temperature (which is here marginal in the RG sense). For comparison, the stiffness exponents for 2D and 3D spin glasses are $\theta_{\mathrm{SG2D}} = -0.28 \pm 0.01$ and $\theta_{\mathrm{SG2D}} = 0.3 \pm 0.1$, respectively (and thus characterized by a $T = 0$ fixed point), whereas for disordered Ising or Potts ferromagnets, $\Delta E \sim L^{d-1}$.

1.3. The method

The ground states of (1), i.e. the configuration $\mathbf{n}^0 = (n_1^0, \ldots, n_N^0)$ with the lowest value for the energy $H[\mathbf{n}^0]$ for a given disorder configuration $\mathbf{d} = (d_1, \ldots, d_N)$, can be computed very efficiently using a minimum cost flow algorithm [36, 16, 37]. For the specific details of how domain walls are induced in the ground state it is useful to recapitulate the mapping onto a minimum cost flow problem.

After introducing the height differences $n_{ij}^* = n_i - n_j$ (integer) and $d_{ij}^* = d_j - d_i$ ($\in[-1, +1]$) along the links $k = (i, j)$ on the dual lattice G^* one obtains a cost (or energy) function that lives on the dual lattice:

$$H[\mathbf{n}^*] = \sum_k (n_k^* - d_k^*)^2. \tag{7}$$

The configurations $\mathbf{n}_k^* = (n_1^*, \ldots, n_M^*)$, where M is the number of links (or bonds) of the original lattice, constitute a 'flow' on the graph G^*. Suppose the original model (1) has

J. Stat. Mech. (2009) P08022

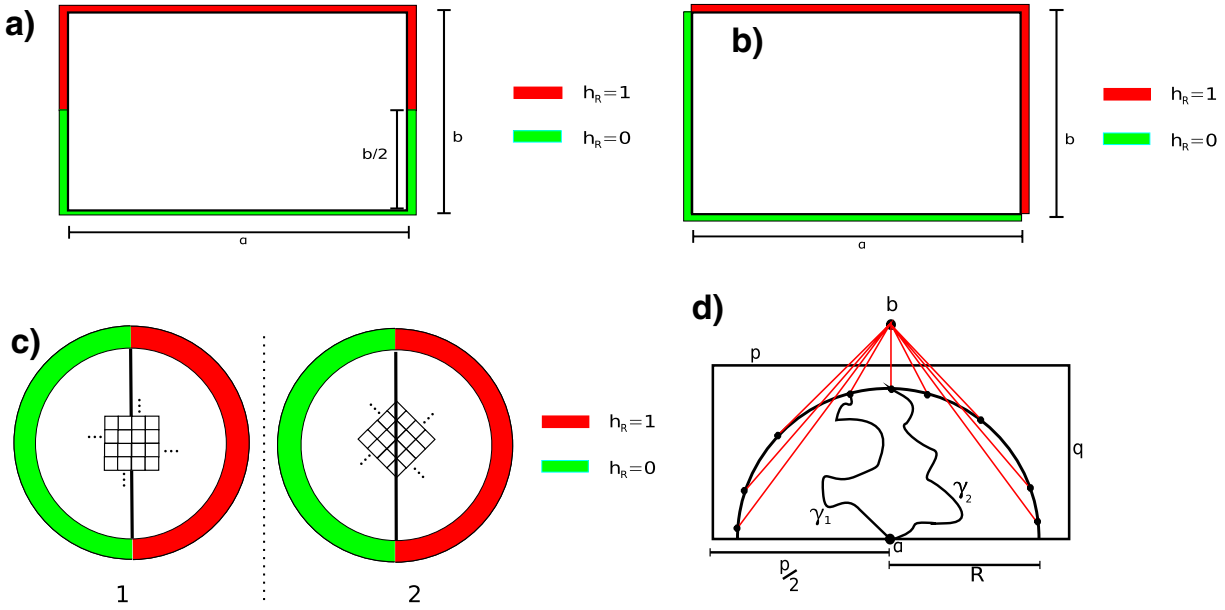

Figure 2. Different geometries and constraints on domain walls considered here. (a) Boundary conditions inducing a step/domain wall as in figure 1. (b) Boundary conditions inducing a step/domain wall running diagonally from one corner of the rectangular lattice to the opposite one. (c) Boundary conditions for a circular domain inducing a boundary along the equator with two different orientations of the underlying lattice. (d) Boundary conditions for a half-circle domain and a domain wall with one fixed end at the origin and a free end on the outer half-circle.

free boundary conditions. Then the sum of the height differences along any directed cycle in the original lattice vanishes. Therefore the divergence of $\mathbf{n}^*$ vanishes at all sites i:

$$(\nabla \cdot \mathbf{n}^*)_i = 0, \tag{8}$$

which means that the flow $\mathbf{n}^*$ on G^*, in order to give rise to a height field $\mathbf{n}$ on the original lattice G, has to be divergenceless, i.e. without sources or sinks. The problem of determining the ground state $\mathbf{n}$ of (1) is thus equivalent to that of finding the flow $\mathbf{n}^*$ with the minimum cost (7) under the mass-balance constraint (8)—i.e. a minimum cost flow problem, for which there exist very powerful algorithms [36, 16, 37].

Enforcing one domain wall, or step of height 1, in the ground state of (1) by means of an appropriate boundary condition is then equivalent to modifying the constraint (8) at exactly two sites, the start and end points of the domain wall (see figures 2(a)–(d)). As an example consider the case in which one wants the domain wall to start at the point $(x, y) = (1, L/2)$ and end at $(x, y) = (L, L/2)$ in a square lattice. Then one chooses the boundary conditions for n_i as follows (cf figure 2(a)): one fixes the values for n_i at the lower half of the boundary (i.e. at $i = (x, 1)$ for $x = 1, \ldots, L$ and $i = (1, y)$ and (L, y) for $y = 1, \ldots, L/2$) at $n_i = 0$, and the values for n_i at the upper half of the boundary (i.e. at $i = (x, L)$ for $x = 1, \ldots, L$ and at $i = (1, y)$ and (L, y) for $y = L/2 + 1, \ldots, L$) at $n_i = 1$. Translating these boundary conditions for the height variables $\mathbf{n}$ into constraints for the flow variables $\mathbf{n}^*$, one immediately sees that at the points $(x, y) = (1, L/2)$ and

$(x, y) = (L, L/2)$, where the step in the height profile starts and terminates, respectively, the constraint (8) is modified into

$$(\nabla \cdot \mathbf{n}^*)_{(1,L/2)} = +1, \qquad (\nabla \cdot \mathbf{n}^*)_{(L,L/2)} = -1. \tag{9}$$

In other words: the induced step sends a unit of flow from the starting point of the domain wall, hence being a source of unit strength, across the sample to the end point, the sink, along an optimal (minimum cost/energy) path. In what follows we identify domain walls immediately with the optimal path for the extra flow unit defined by the modified mass-balance constraints (9).

With the help of this concept one can then also consider situations in which the starting point of the domain wall is fixed but the ending is only forced to be on a specific region of the boundary, opposing the starting point (see figure 2(d)). Suppose one wants the domain wall to start at $i_s = (1, L/2)$, and terminate somewhere on the opposing boundary $i_t = (L, y)$ with $y \in \{1, \ldots, L\}$. Then one introduces an extra node into the dual graph G^*, denoted as the target node, connects it with bonds of zero cost to all sites on the terminal boundary, and assigns a sink strength -1 to it. The source node is the one closest to i_s in the dual graph and has source strength $+1$. The minimum cost flow of this arrangement is then the desired ground state configuration with a domain wall starting at i_s and ending somewhere on the opposite boundary.

2. Schramm–Loewner evolution (SLE)

Since the domain walls as defined above represent fractal curves embedded in a two-dimensional space, the question arises of whether they fall into the classification scheme of Schramm–Loewner evolution (SLE) like loop-erased random walks, percolation hulls, and domain walls at phase transitions in 2D in the scaling limit [22, 21]. The necessary (and sufficient) condition for a set of random curves connecting two points on the boundary D of a domain to be described as showing SLE are (1) the measure for these random curves has to obey a Markov property, (2) the measure has to be invariant under conformal mappings of the domain. Recently it was suggested that domain walls in 2D spin glasses can also be described as showing SLE [23, 24], although the conformal invariance requirement is not fulfilled for each individual disorder realization and also the Markov property is not obeyed after disorder averaging. However, conformal invariance might hold for the disorder averaged model and the Markov property might be obeyed almost always in a statistical sense.

A single parameter κ parameterizes all SLEs and it is related to the fractal dimension of the curve via

$$d_s = 1 + \kappa/8. \tag{10}$$

The parameter κ is the diffusion coefficient of the Brownian motion that underlies the SLE and generates via a random sequence of simple conformal maps the fractal curves. In addition to the fractal dimension it determines various other geometric and statistical properties of the SLE curves. One of them is that the probability that a curve in the upper half-plane $\mathbb{H}$ generated by SLE will pass to the left of a given point $z = x + iy$ is

J. Stat. Mech. (2009) P08022

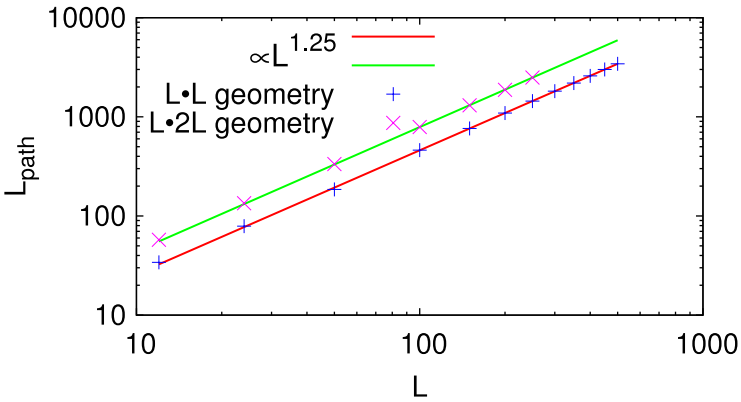

Figure 3. Average length of domain walls spanning the system from one end to the opposite one as a function of the system size L in a log–log plot. The straight lines are least square fits to (5) and yield the estimate for the fractal dimension $d_s = 1.25 \pm 0.01$.

given by Schramm's 'left passage formula' [38]

$$P_\kappa(z) = \frac{1}{2} + \frac{\Gamma(4/\kappa)}{\sqrt{\pi}\,\Gamma((8-\kappa)/2\kappa)}\,{}_2F_1\left(\frac{1}{2}, \frac{4}{\kappa}; \frac{3}{2}; -\left(\frac{x}{y}\right)^2\right)\frac{x}{y}, \tag{11}$$

where ${}_2F_1$ is the hypergeometric function: ${}_2F_1(a_1, a_2; b; z) = \sum_{k=0}^{\infty}(\Gamma(k+a_1)/\Gamma(a_1))(\Gamma(k+a_2)/\Gamma(a_2))(\Gamma(b)/\Gamma(k+b))(z^k/k!)$. Since the probability depends just on the ratio between $\mathrm{Re}(z)$ and $\mathrm{Im}(z)$, it is sometimes useful to replace this ratio by a function of an angle. We decided to use $\tan(\phi) = x/y$. So $\phi \in]-(\pi/2); (\pi/2)[$ is the angle at the origin between the imaginary axis and z. This formula holds for the domain of the SLE being the upper half-plane with the start point of the curve being identical to the origin of the coordinate system and the end point at infinity.

A standard check of whether an ensemble of random curves is a potential candidate for showing SLE therefore is to simultaneously determine their fractal dimension d_s and the left passage probabilities, and to test whether the latter fit (11) with $\kappa = 8(d_s - 1)$ [23]–[25].

In figure 3 we show our data for the average length of a domain wall in the configuration depicted in figure 2(b), i.e. starting at the point $i_s = (1, 1)$ and ending at $i_t = (L, L)$ in an $L \times L$ geometry and at $i_t = (L, 2L)$ in an $L \times 2L$ geometry. Least square fits to the scaling law (5) yield the estimate $d_s = 1.25 \pm 0.01$ which agrees with the value found in [18].

This value for the fractal dimension would imply $\kappa = 2.00 \pm 0.08$ if the domain walls could be described as showing SLE. Next we determined for different points (x, y) of the lattice the frequency that a domain wall passes to the left of it, yielding a probability $p(x, y)$, which we compared with Schramm's left passage formula $P_\kappa(x, y)$ for fixed κ. For the circle domain and the choice of the start and end points of the domain wall as shown in figure 2(c), the formula (11) is modified.

Let $\mathbb{E}$ be the unit circle in the complex plane. The Cayley function $g: \mathbb{E} \to \mathbb{H}, z \mapsto i((1+z)/(1-z))$ maps the unit circle conformally into the upper half-plane $\mathbb{H}$. Furthermore $g(-1) = 0, g(1) = \infty$; thus curves in $\bar{\mathbb{E}}$ starting at $z = -1$ and ending at $z = 1$ are conformally mapped onto curves in $\bar{\mathbb{H}}$. For the latter, if the curves are described

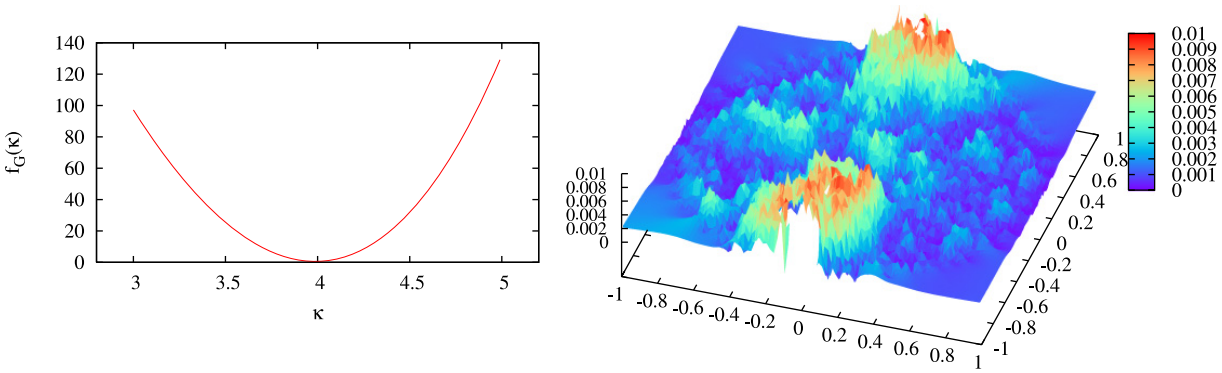

Figure 4. Left: the cumulative squared deviation $f_G(\kappa)$ of the computed left passage probabilities $p(x, y)$ from the values $P_{\kappa,g}(x, y)$ given by (12) as a function of κ. The underlying lattice geometry is the circle as sketched in figure 2(c); the corresponding conformal map $g(z)$ entering (12) is given in the text. The minimum is at $\kappa = 4.00 \pm 0.01$ with a squared difference per grid point of about 2×10^{-5}. Right: absolute difference between the calculated left passage probability $p(x, y)$ and the SLE expectation $P_{\kappa,g}(x, y)$ (12) for $\kappa = 4$ as a function of the 2D lattice coordinates (x, y). For the whole unit circle the deviation is almost everywhere smaller than 1%. Note that the domain wall is fixed at $(-1, 0)$ and $(1, 0)$, where the largest deviations occur.

as showing SLE, Schramm's formula (11) holds, so for the former, the modified formula

$$P_{\kappa,g}(z) = \frac{1}{2} + \frac{\Gamma(4/\kappa)}{\sqrt{\pi}\,\Gamma((8-\kappa)/2\kappa)}\,{}_2F_1\left(\frac{1}{2}, \frac{4}{\kappa}; \frac{3}{2}; -\left(\frac{\mathrm{Re}\, g(z)}{\mathrm{Im}\, g(z)}\right)^2\right)\frac{\mathrm{Re}\, g(z)}{\mathrm{Im}\, g(z)} \tag{12}$$

holds. Hence we filled the unit circle with finer and finer grids G approximating better and better the continuum limit for the curves in $\mathbb{E}$ that we want to check for SLE. For this we define the function

$$f_G(\kappa) = \sum_{(x,y)\in G} [p(x, y) - P_{\kappa,g}(x, y)]^2 \tag{13}$$

that measures the cumulative squared deviation of the probabilities $p(x, y)$ from the SLE value for given κ. The result is shown in figure 4. The minimal deviation of the data from the expected SLE result is at $\kappa = 4.00 \pm 0.01$ which clearly differs from the value $\kappa = 2.00 \pm 0.08$ that one would expect from the fractal dimension if the domain walls were to be described as showing SLE.

Next we varied the geometry and the domain wall constraints and studied the case depicted in figure 2(b), i.e. a quadratic domain D with corners at 0, p, $p + \mathrm{i}p$, $\mathrm{i}p$ (p real and positive). The function $g\colon D \to \mathbb{H}\colon z \mapsto -\mathfrak{p}(z; S)$ with $S = \{2n_1 p + \mathrm{i}2n_2 p |\, n_1, n_2 \in Z\}$ defines a conformal map from D into $\mathbb{H}$, where $\mathfrak{p}(z; S) = (1/z^2) + \sum_{\omega\in S\setminus\{0\}}[(1/(z-\omega)^2) - (1/\omega^2)]$ is the Weierstrass $\mathfrak{p}$-function. Furthermore $g(p + \mathrm{i}p) = 0, g(0) = \infty$; thus curves in $\bar{D}$ starting at $z = 0$ and ending at $z = p + \mathrm{i}p$ are conformally mapped onto curves in $\bar{\mathbb{H}}$ starting at the origin and extending to infinity. Using g in (12) we determined κ in the same way as in the case of the unit circle. The result is shown in figure 5 and yields $\kappa = 4.00 \pm 0.01$.

doi:10.1088/1742-5468/2009/08/P08022

J. Stat. Mech. (2009) P08022

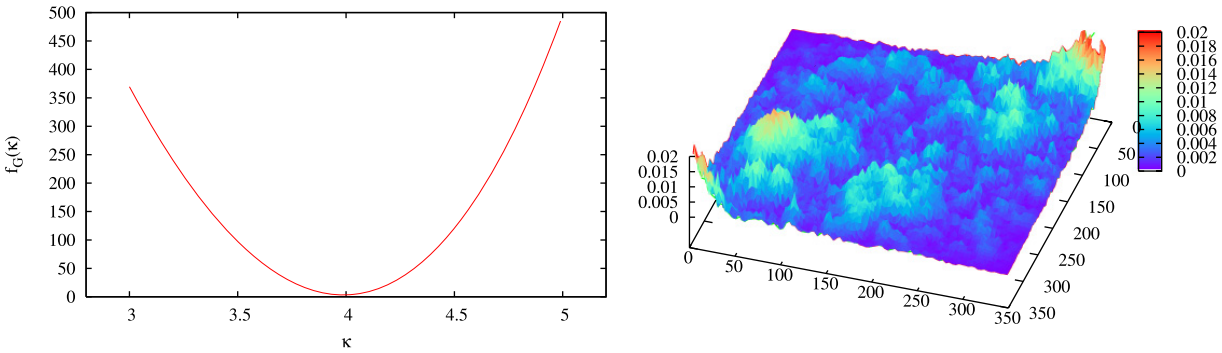

Figure 5. Cumulative deviation $f_G(\kappa)$ as a function of κ and absolute difference between $p(x, y)$ and $P_{\kappa,g}(x, y)$ for $\kappa = 4$ as in figure 4 but for the square geometry as depicted in figure 2(b). Note that the domain wall is fixed at $(0, 0)$ and (L, L), where the largest deviations occur.

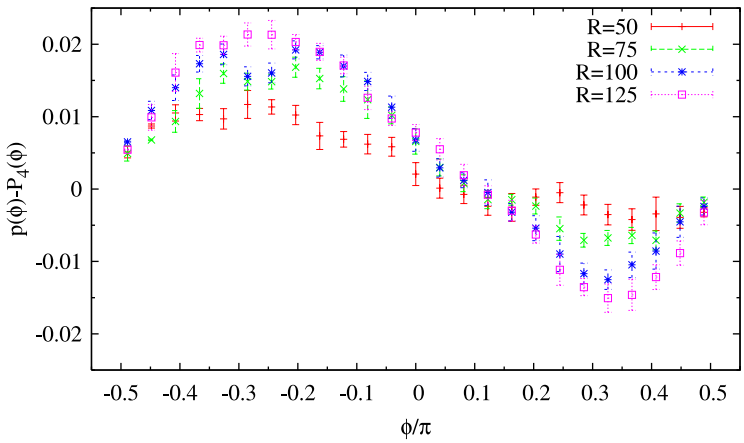

Figure 6. Deviation of the left passage probability $p(\phi)$ from the SLE expectation $P_\kappa(\phi)$, (11), for $\kappa = 4$ in the half-circle geometry depicted in figure 2(d) $(p = 510, q = 255, R = 500)$, i.e. one free end of the domain wall.

We also compared $p(x, y)$ directly with $P_{\kappa=4}(x, y)$ for curves in the upper half-plane $\mathbb{H}$ starting at the origin. For this we considered the geometry depicted in figure 2(d), in which the curves starting at the origin can end anywhere on the half-circle. We checked the prediction (11) for different radii R and angles $\Phi = \arctan(x/y) \in]-(\pi/2); (\pi/2)[$. The result is shown in figure 6, where the deviations from $P_\kappa(\phi)$, (11), for $\kappa = 4$ are everywhere less than 2% for the size $L = 500$ and radii shown in figure 6. We also observe that the deviation systematically decreases with the system size L for fixed ratio R/L, indicating vanishing deviations $P(\Phi) - P_{\kappa=4}(\Phi)$ in the limit $L \to \infty$.

For all the geometries with domain walls starting at a fixed point that we studied, we found that the data can be nicely fitted with $\kappa = 4$, but the fractal dimension of the domain walls is unchanged for the different set-ups: $d_s = 1.25 \pm 0.01$. The conclusion is that domain walls in the SOS model on a disordered substrate *cannot* be described as showing SLE. A question arises: Which condition for SLE is actually violated? The fact that for all geometries the left passage probability that we studied can be well represented by a

J. Stat. Mech. (2009) P08022

common expression, Schramm's formula, containing the conformal map of the half-plane to the specific geometry under consideration, would actually hint at conformal invariance. But obviously this does not exclude the possibility that a breaking of conformal invariance manifests itself in other quantities, or even other geometries. We did not attempt to check the domain Markov property, as was tried in [24].

Finally we checked whether domain walls with both ends *not* fixed can be described as showing SLE, as was reported for 2D spin glasses in [23, 24]. In the SOS model on a square lattice this is realized by connecting one side (or a central part of it) to the source and the opposite to the sink. The algorithm will automatically find the optimal entry and exit points of the additional flow unit, i.e. the optimal end points of the domain wall on the two opposing boundary sides (cf [18]). To avoid the influence of the boundary perpendicular to the entry and exit we used a $2L \times L$ geometry and connected only the central part of length L of the long ($2L$) sides to the source and sink, respectively. To determine the left passage probabilities $p(\phi)$ we define for each individual sample the entry point of the domain wall as the origin of the coordinate system. As a result we find that now the value for κ that yields the best fit of Schramm's formula to the left passage probabilities is changed to $\kappa \approx 3$, but the fractal dimension is still $d_{\mathrm{f}} = 1.25 \pm 0.01$ (cf [18]). Therefore we conclude that also boundary conditions with free domain wall start and end points do not show SLE.

3. Excitations

In this section we study large scale excitations that cost a minimum amount of energy, also denoted as droplets [2], and the size dependence of their energy. According to the usual arguments in droplet scaling theory [2] this excitation energy is expected to scale in the same way as a domain wall of lateral size L, i.e. like $\Delta E \sim L^{\theta}$ with θ the stiffness exponent, which for the system that we consider is $\theta = 0$. The domain wall energy scales as $\Delta E_{\mathrm{DW}} \sim \log L$ (cf (6)), and if it is correct that all excitations of scale L display the same behavior then a question arises: How can thermal fluctuations destabilize the ground state such that the present model is indeed characterized by a line of fixed points, indexed by temperature (and thus different from a $T = 0$ fixed point like for spin glasses with $d > 2$)? A $\log L$ scaling of excitations still implies that larger and larger excitations, needed to occur to decorrelate the system's state from the ground state, need more and more energy and are therefore more and more unlikely, i.e. occurring with a probability that decays as $\exp(-\Delta E_{\mathrm{DW}}/T) \sim L^{-c/T}$ at $T > 0$.

The solution to this problem lies in the freedom that domain walls of excitations of scale L have to optimize their energy (cf a similar discussion in the context of optimized dislocations in [18]). Finding the optimal excitation of a given scale requires a greater effort than searching for a domain wall with given start and end points (as we have seen above, there are even efficient ways to optimize the positions of these end points). There is a simple way to induce excitations of an *arbitrary* scale, as first proposed in the context of spin glasses [4] and used again in [8]: we could compute the ground state for fixed boundary conditions as depicted in the left panel of figure 1; this yields $\mathbf{n}^0$. Then we choose a central site (say $i = (x, y) = (L/2, L/2)$), fix it to $n_i = n_i^0 + 1$, fix the boundary as before and compute the ground state again, giving $\tilde{\mathbf{n}}^0$. This will differ from $\mathbf{n}^0$ only by a compact cluster C that contains the site i and which has $\tilde{n}_i^0 = n_i^0 + 1$. This is then in

J. Stat. Mech. (2009) P08022

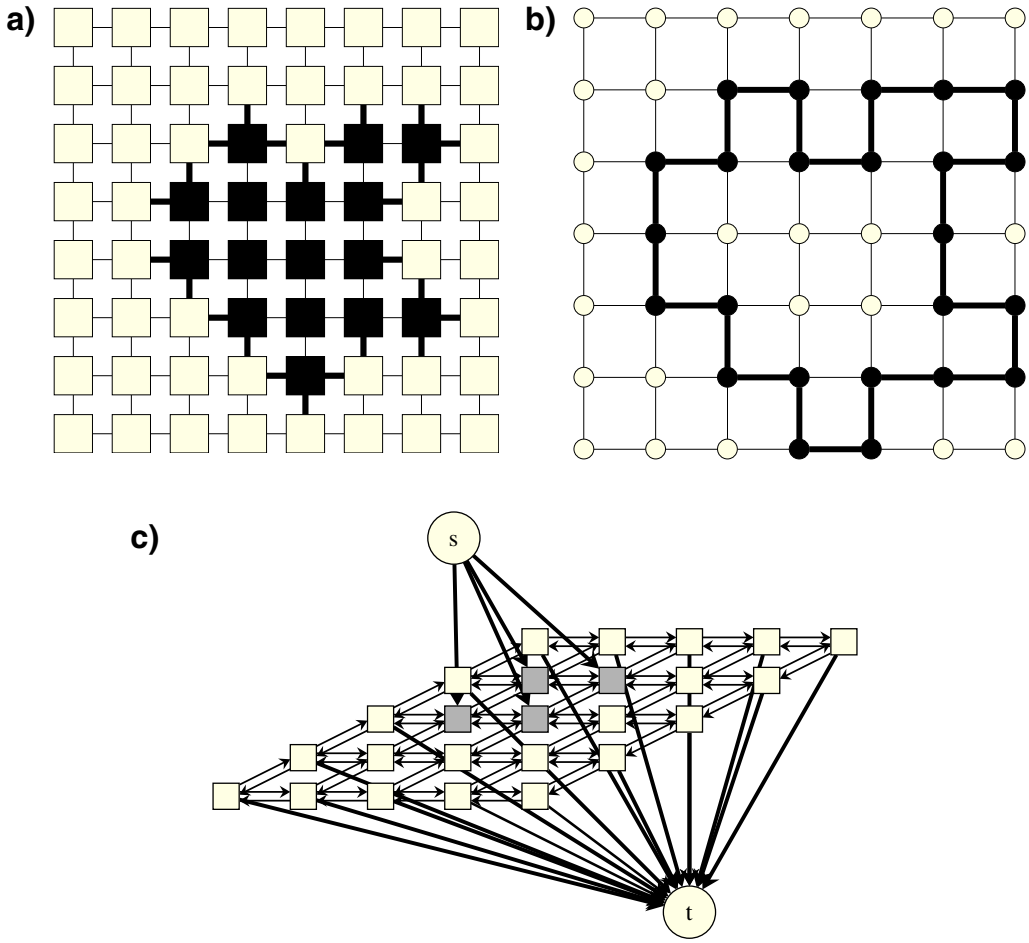

Figure 7. (a) Sketch of a droplet excitation representing a simply connected cluster $\mathcal{C}$ of sites i whose height values are increased by 1 as compared to the ground state: $n_i = n_i^0 + 1\,\forall i \in \mathcal{C}$. (b) Directed cycle in the dual lattice corresponding to the cluster in (a) representing the step in height profile induced by raising the cluster $\mathcal{C}$ by one height unit. (c) Sketch of an s–t cut of the nodes of the original lattice graph such that those sites connected to the external node s are forced to be in the set S and those connected to t, in the set T (see the text).

fact an optimal or droplet excitation, but its size $V = \#\{i \in C\}$ can vary from 1 to L^2. Droplets of a *fixed* size cannot be generated in this way.

The SOS model on a disordered substrate actually allows for an efficient search for optimal excitations of a given scale, as we describe in the following.

A droplet excitation in the SOS model is a simply connected cluster $\mathcal{C}$ of sites whose height values are all increased (or all decreased) by 1 as compared to the ground state: $n_i = n_i^0 + 1\,\forall i \in \mathcal{C}$; see figure 7. Pictorially it is, in the height representation, an extra mountain (valley) of height $+1$ (-1). Its boundary is a directed cycle in the dual lattice, and remembering the mapping to the minimum cost flow problem (7)–(8), adding a cycle to a feasible solution maintains the divergence-free constraint (8). Hence, the transition from one state to the other is determined by such a cycle. Thus first one has to compute

J. Stat. Mech. (2009) P08022

the ground state of a given disorder realization. Then in order to find a droplet excitation of this ground state that has a given lateral size one can for instance force this extra cycle to run within an annulus of inner radius $L/4$ and outer radius $3L/4$ (i.e. its average diameter is $L/2$). This can be achieved by simply removing all sites/bonds outside this annulus and then computing the optimal cycle within this modified graph, the cost for which depends on the ground state configuration and the substrate heights. One assigns costs to each directed edge (ij) that corresponds to the energy cost for increasing the height difference between its left and right sides by one unit [36, 16, 37]:

$$c_{(ij)} = (h_i^0 + 1 - h_j^0)^2 - (h_i^0 - h_j^0)^2 = 2(h_i^0 - h_j^0) + 1, \tag{14}$$

where $h_i^0 = n_i^0 + d_i$. Note that in practice one may use the reduced costs emerging from the ground state. That is, if and only if a feasible flow has minimum energy, then there are non-negative reduced costs such that the cost of each cycle remains unchanged. If the successive shortest path algorithm is used to solve the minimum cost flow problem when computing the ground state $\mathbf{n}^0$, then no extra work is necessary to compute the desired non-negative reduced costs. Hence, Dijkstra's shortest path algorithm can be used to find the shortest directed cycle around the annulus, i.e. the one separating the inner and outer rings of the annulus. To this end, the annulus is cut from the outer to the inner ring, i.e. the corresponding edges are removed from the graph, to prevent the shortest path from short-cutting. For each of these removed edges, the shortest path from its head to its tail is computed, where only the remaining edges are used. The shortest paths obtained are completed with the corresponding directed edges to form cycles around the annulus. This procedure has to be repeated for all (or a representative number of) positions of the annulus within the original lattice (in practice one fixes the annulus and shifts the disorder configuration, wrapping it around a toroidal geometry).

The procedure of finding the optimal cycle in a given annulus can be simplified by observing that the droplet excitation in the height representation corresponds to an s–t cut of the underlying graph [37][5] in such a way that one forces all nodes of the inner circle of the annulus to belong to S and all nodes of the outer ring of the annulus to belong to T; see figure 7(c). The minimum s–t cut with respect to the non-negative reduced edge costs of the ground state $\mathbf{n}^0$ is then exactly the boundary of the optimal excitation (or the optimal cycle) that one is searching for, for a given annulus arrangement. According to the famous 'min cut–max flow' theorem, one can compute the minimum s–t cut in polynomial time by solving the associated maximum flow problem [16, 37]. We have implemented this procedure and show for illustration a number of examples in figure 8.

Figure 9 shows our result for the disorder averaged energy of the optimal excitations of scale L that we obtain with the procedure described above. This represents an upper bound for the optimal excitations of scale L since the annulus arrangement does not include all possible excitations of scale L. As one can see, this bound saturates at a finite energy of order $\mathcal{O}(1)$ in the limit $L \to \infty$. Consequently arbitrarily large excitations exist that cost only a small amount of energy, which renders the ground state unstable at a non-vanishing temperature.

Figure 10 shows the distribution of optimal excitation energies for different values of L. As can be seen, the distribution is nearly Gaussian with a finite width, i.e. it

[5] An s–t cut is a partition of the nodes of a graph $\mathcal{G}$ into two disjoint sets $\mathcal{S}$ and $\mathcal{T} = \mathcal{G}/\mathcal{T}$ such that $s \in S$ and $t \in T$.

J. Stat. Mech. (2009) P08022

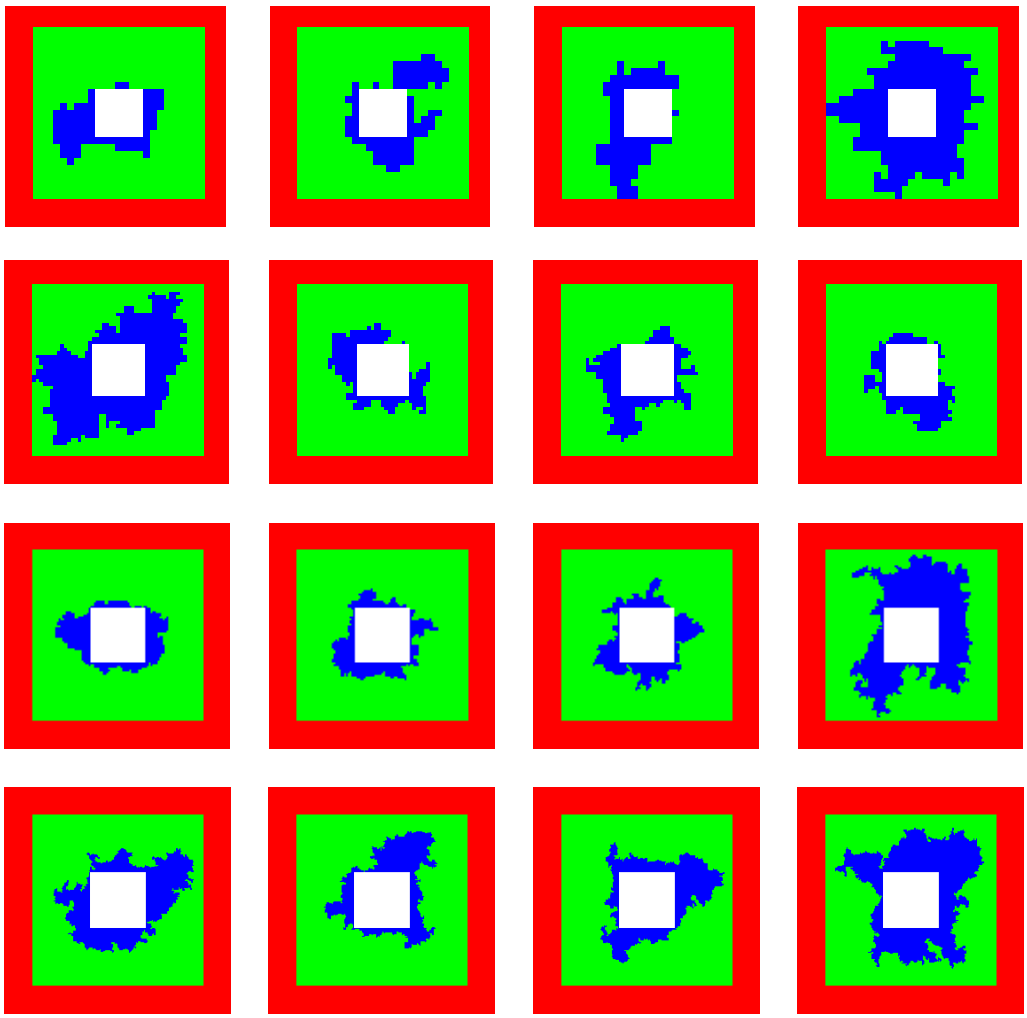

Figure 8. Examples of optimal excitations of scale L, whose boundary (domain wall) is forced to lie in the interior of the area indicated in green (an annulus in square geometry). From the top row to the bottom we have $L = 32$, 64, 128 and 256. Pictures are scaled to have the same size.

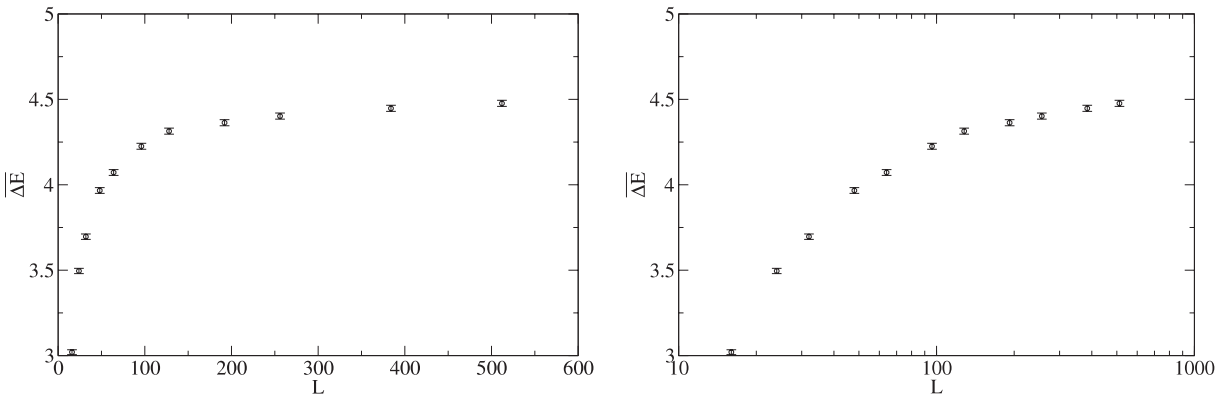

Figure 9. Disorder averaged energy of the optimal excitations of scale L as a function of L—left on a linear scale, right on a log–log scale.

doi:10.1088/1742-5468/2009/08/P08022

J. Stat. Mech. (2009) P08022

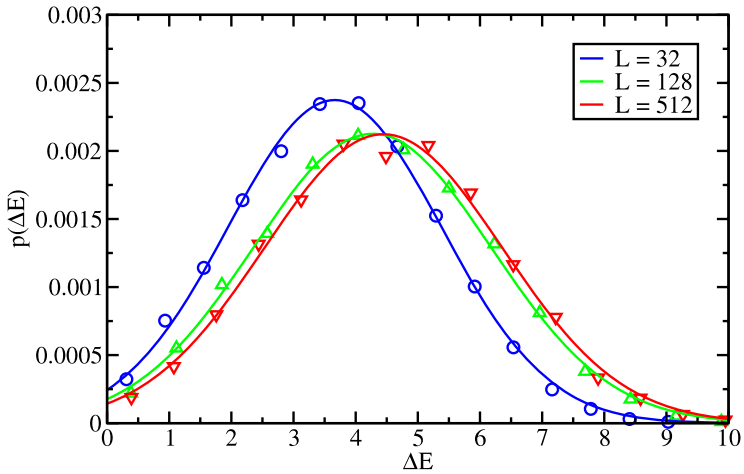

Figure 10. Distribution of the optimal excitation energies of scale L for three values of L. For $L \geq 128$ this distribution becomes independent of L.

does not display long, e.g. algebraically decaying, tails, which implies that the average is representative for almost all disorder configurations. It can also be seen that the whole probability distribution $P_L(\Delta E)$ becomes independent of the length scale L for large L. This is an important observation since from droplet scaling theory [2] one would expect $P_L(\Delta E) \sim l^{-\theta}\tilde{p}(\Delta E/L^{\theta})$. For $\theta = 0$, as is the case here, it is not *a priori* clear whether this implies $P_L(\Delta E) \sim (\ln L)^{-1}\tilde{p}(\Delta E/\ln L)$, i.e. a scaling with the average domain wall energy $\ln L$, or $P_L(\Delta E) \sim \tilde{p}(\Delta E)$, i.e. droplet size independence. Figure 10 shows that the latter is correct.

This has important implications for the scaling of the average droplet energy within a system of lateral size L as determined in [20]. There the average energy of droplets of size $l < L$, $(\Delta E)_L^{\min}$, i.e. without a lower bound, was estimated to behave like $(\Delta E)_L^{\min} \sim \ln L$. In order to make contact with our result one should note that this energy is the minimum among droplets of the kind that we determined here, with size $l \in [L/2, L]$, $l \in [L/4, L/2]$, $l \in [L/8, L/4]$, ..., i.e. a minimum of approximately $\ln L$ random numbers. Only if the probability distribution of these energies is (a) independent and (b) identically distributed does their minimum go like the inverse of their number, i.e. $(\Delta E)_L^{\min} = \min\{(\Delta E)_{L/2^1}, (\Delta E)_{L/2^2}, \ldots, (\Delta E)_{L/2^k}\} \sim 1/k$ with $k \sim \ln L$. According to our result depicted in figure 10 the assumption b, which is implicit in the reasoning of [20], is indeed fulfilled.

Finally we note that we also determined the fractal dimension of the boundary of the optimal excitations and found that it is identical to the fractal dimension of the domain walls with fixed start and end points: $d_s = 1.25 \pm 0.01$.

4. Disorder chaos

In this section, we study the sensitivity of the ground state to a small change of the quenched disorder configuration. To this end we generate a configuration of random offsets d_i^1 and compute the associated ground state h_i^1. Then we slightly perturb this configuration of random offsets $d_i^2 = d_i + \delta\epsilon_i$ with $\delta \ll 1$ and where the ϵ_is are independent

J. Stat. Mech. (2009) P08022

and identically distributed Gaussian variables of unit variance, and we compute the associated ground state h_i^2. The question that we ask is: How different are these two configurations of the systems h_i^1 and h_i^2?

Such questions first arose in the context of spin glasses [1], where it was proposed that disorder induced glass phases may exhibit 'static chaos', i.e. extreme sensitivity to such small modifications of external parameters (like disorder, considered here, or temperature). Such small perturbations are argued to decorrelate the system beyond the so called *overlap length* L_δ which diverges for small δ as $L_\delta \sim \delta^{-1/\alpha}$, with α the chaos exponent. As an example let us first consider the case of an Ising spin glass with a continuous Gaussian distribution of random exchange interactions, of width J. The system has two ground states related by a global spin reversal. Within the phenomenological droplet theory [1, 14, 41], a low-lying energy excitation of the system involves an overturned droplet of linear size L and costs an energy JL^θ. If we now add a small random bond perturbation, say Gaussian of width δJ, the excess energy of a droplet is modified. For such a spin glass system, this energy comes only from the bonds which are at the *surface* of the droplet. Their contribution is thus the sum of L^{d_s} independent random variables of width δJ, where d_s is the fractal dimension of the droplet: it is thus of order $\pm\delta\ell^{d_s/2}$. Therefore the ground state is unstable against perturbation on length scales L such that $\delta J L^{d_s/2} > JL^\theta$, i.e. $L > L_\delta$ where $L_\delta \sim \delta^{-1/\alpha_{SG}}$ with $\alpha_{SG} = d_s/2 - \theta$. One thus sees that, for spin glasses, disorder chaos is closely related to the (geometrical) properties of the domain walls.

The situation is rather different for elastic systems in a random potential as considered here. Here we consider the SOS model on a disordered substrate defined in equation (1) as

$$H = \sum_{(ij)} (h_i - h_j)^2, \qquad h_i = n_i + d_i, \tag{15}$$

with $i \equiv (x_i, y_i) \in \mathbb{Z}^2$. In equation (15) the height variables n_i $(i = 1, \ldots, N)$ take on integer values $n_i = 0, \pm 1, \pm 2, \ldots$ and the offsets d_i are independent quenched random variables uniformly distributed between 0 and 1. This system (with free or periodic boundary conditions) has infinitely many ground states which differ by a global shift $\Delta n \in \{\pm 1, \pm 2, \ldots\}$. Again, within the droplet argument [14, 42, 43] a low-lying energy excitation of the system involves a droplet of size L where the height field is shifted by unity, say $\Delta n = 1$, and it costs an energy L^θ. But now if we had a small perturbation $d_i^2 = d_i^1 + \delta\epsilon_i$, the excess energy of this droplet would come from the *bulk* of the droplet, which experiences a random force field. This contribution is thus the sum of L^d random variables of width δ and therefore in this case the ground state is unstable against the perturbation on length scales $L > L_\delta$ where $L_\delta \sim \delta^{-1/\alpha}$ with $\alpha = d/2 - \theta$. Here $d = 2$ and $\theta = 0$ and thus one expects $L_\delta \propto \delta^{-1}$. At variance with the case of spin glasses discussed above, one thus sees that for disordered elastic systems, disorder chaos is not directly related to the properties of domain walls.

For the present model (15), disorder chaos was demonstrated analytically at finite T near the glass transition T_g using a Coulomb gas renormalization group [44]. At $T = 0$, some indications of disorder chaos were also found numerically in [16] where global correlations between h_i^1 and h_i^2 were studied through $\chi(\delta) = \sum_i (h_i^1 - h_i^2)^2$. In this paper, following [43], we characterize the local correlations between these two configurations

J. Stat. Mech. (2009) P08022

using the correlation function $C_{ij}(\mathbf{r})$ with $\mathbf{r} \equiv (x, y)$ (with $i, j = 1, 2$):

$$C_{ij}(\mathbf{r}) = \overline{(h^i_k - h^i_{k+\mathbf{r}})(h^j_k - h^j_{k+\mathbf{r}})}, \tag{16}$$

where $k+\mathbf{r} \equiv (x_k+x, y_k+y)$ and for the rotationally invariant system considered here one has $C_{ij}(\mathbf{r}) \equiv C_{ij}(r)$ with $r = |\mathbf{r}|$. In the following we will talk about *intralayer* correlations for $C_{ii}(r)$ and *interlayer* correlations for $C_{i\neq j}(r)$. Equivalently, one can also study such correlations (16) in Fourier space and define $S_{ij}(\mathbf{q})$ with $\mathbf{q} \equiv (q_x, q_y)$ as

$$S_{ij}(\mathbf{q}) = \overline{\hat{h}^i_q \hat{h}^j_{-q}}, \qquad \hat{h}^j_q = \frac{1}{L^2} \sum_k h^j_k \mathrm{e}^{\mathrm{i}\mathbf{q}\cdot k}, \tag{17}$$

where $\mathbf{q} \cdot k = q_x x_k + q_y y_k$. For the rotationally invariant system considered here, one has $S_{ij}(\mathbf{q}) \equiv S_{ij}(q)$ where $q = |\mathbf{q}|$.

Disorder chaos at $T = 0$ in generic disordered elastic systems in dimension d was recently studied analytically using the functional renormalization group (FRG) [43]. At one-loop order in a dimensional expansion in $d = 4 - \epsilon$ it was found that for short range disorder (like in random bond problems) and random periodic systems in dimension $d > 2$ (including one-component Bragg glass), one has [43]

$$C_{12}(r) = r^{2\zeta} \Phi(\delta r^\alpha) \qquad \text{with } \Phi(x) \sim \begin{cases} c^{\mathrm{st}}, & x \ll 1, \\ x^{-\mu}, & x \gg 1, \end{cases} \tag{18}$$

with c^{st} a constant, ζ the roughness exponent and where μ is the *decorrelation* exponent. Translated into Fourier space, this yields

$$S_{12}(q) = L_\delta^{(d+2\zeta)} \varphi(q L_\delta) \qquad \text{with } \varphi(x) \sim \begin{cases} x^{-d-2\zeta+\mu}, & x \ll 1, \\ x^{-d-2\zeta}, & x \gg 1, \end{cases} \tag{19}$$

with $L_\delta \sim \delta^{-1/\alpha}$ and where the behavior for large x is then such that the dependence on L_δ cancels in this limit, as it should.

The two-dimensional disordered SOS model that we are considering here (15) corresponds precisely to the marginal case $d = 2$ (with $\zeta = 0$ and thus $\theta = 0$) where, as discussed in [43, 45], the analysis yielding the result in equation (18) ceases to be valid. Indeed in that case non-local terms, irrelevant for $d > 2$, are generated under coarse-graining and these additional terms have to be handled with care at $T = 0$. One thus considers the Hamiltonian associated with the two copies of the system parameterized by the scalar fields $u^i \equiv u^i(\mathbf{r})$:

$$H_{2\,\mathrm{copies}} = \frac{1}{T} \sum_{i=1,2} \int \mathrm{d}^2\mathbf{r} \left[\frac{1}{2} (\nabla_{\mathbf{r}} u^i)^2 + V_i(u^i, \mathbf{r}) - \boldsymbol{\mu}^i(\mathbf{r}) \cdot \nabla_{\mathbf{r}} u^i \right], \tag{20}$$

where $\boldsymbol{\mu}^i \equiv (\mu^i_x, \mu^i_y)$ are two-component random tilt fields, which are generated upon renormalization. While they are irrelevant for $d > 2$, they become relevant for $d = 2$ where they play a crucial role. These two copies u^1, u^2 are thus independent of (20), but they feel two mutually correlated random potentials

$$\overline{V_i(u, \mathbf{r}) V_j(u', \mathbf{r}')} = R_{ij}(u - u') \delta^2(\mathbf{r} - \mathbf{r}'), \tag{21}$$

$$\overline{\mu^i_\rho(\mathbf{r}) \mu^j_{\rho'}(\mathbf{r}')} = \sigma_{ij} \delta_{\rho\rho'} \delta^2(\mathbf{r} - \mathbf{r}'), \tag{22}$$

J. Stat. Mech. (2009) P08022

where $i = 1, 2$ is the index of the copy and $\rho = x, y$ is a spatial index. This leads to a replicated Hamiltonian, $\overline{Z^n} = \exp(-H_{\rm rep})$:

$$H_{\rm rep} = \frac{1}{2T}\int \mathrm{d}^2\mathbf{r} \sum_{i=1}^{2}\sum_{a=1}^{n}\frac{1}{2}(\nabla_{\mathbf{r}} u_a^i)^2 - \frac{1}{2T^2}\sum_{i,j=1}^{2}\sum_{a,b=1}^{n}\int \mathrm{d}^2\mathbf{r}\,[R_{ij}(u_a^i - u_b^j) - \tfrac{1}{2}\nabla_{\mathbf{r}} u_{ab}^i \nabla_{\mathbf{r}} u_{ab}^j G_{ij}(u_a^i - u_b^j)], \tag{23}$$

where we used the notation $u_{ab}^i = u_a^i - u_b^i$. In the 'bare' model, one has $G_{ij}(u) = \sigma_{ij}$.

Close to the transition $T \lesssim T_{\rm g}$, this model (23) was studied using Wilson RG analysis by varying the short scale momentum cutoff $\Lambda_\ell = \Lambda \mathrm{e}^{-\ell}$, with ℓ the log scale. It was shown, using the Coulomb gas technique at lowest order, that $G_{ii} \propto \sigma\ell$. This leads to the correlation function in Fourier space $S_{ii}(q) \propto \sigma\ell/q^2$, which yields, setting $\ell = \log(1/q)$, the $\log^2(r)$ behavior of the intralayer correlations (this result for $C_{ii}(r)$ can be derived in a more controlled way using the exact renormalization group [46]). As regards chaos properties, it was shown in [44] that $G_{12}(0)$ grows linearly with ℓ for small ℓ before it saturates to a constant for large ℓ, $G_{12}(0) \sim \hat{\sigma} > 0$, which yields $S_{12}(q) \propto \hat{\sigma}/q^2$. These results close to $T_{\rm g}$ can be summarized as

$$S_{12}(q) \sim \begin{cases} \sigma\dfrac{\log 1/q}{q^2}, & q \gg L_\delta^{-1}, \\ \dfrac{\hat{\sigma}}{q^2}, & q \ll L_\delta^{-1}, \end{cases} \tag{24}$$

while in real space, the behavior of the interlayer correlation function $C_{12}(r)$ for $T \lesssim T_{\rm g}$ is thus

$$C_{12}(r) \sim \begin{cases} \sigma \log^2(r), & r \ll L_\delta, \\ \hat{\sigma}\log(r), & r \gg L_\delta. \end{cases} \tag{25}$$

At $T = 0$, it was recently shown [34], using the FRG to one-loop order including the term $G_{11}(u)$, that the intralayer correlation function also behaves like $C(r) \propto \log^2(r)$, in rather good agreement with the numerics [16, 32]. One thus also expects to find $C_{12}(r) \propto \log^2(r)$ for $r \ll L_\delta$ [16, 32, 34]. For $r \gg L_\delta$, a behavior of $C_{12}(r) \sim \hat{\sigma}\log r$ as in equation (24) was discussed in [43]. To determine analytically whether $\hat{\sigma} > 0$ at $T = 0$ requires a detailed and difficult analysis of the coupled FRG equations for $R_{ij}(u), G_{ij}(u)$, (23), which goes beyond the previous studies done in that direction in [34, 43, 45]. Here, we will answer this question using numerical simulations.

The purpose of our study is actually to answer two main questions: (i) What are the residual correlations beyond L_δ and, in particular, is $\hat{\sigma}$ also finite at $T = 0$? (ii) What is the scaling form of this correlation function $C_{12}(r)$, i.e. the analogue of equation (18) from which one can extract the overlap length L_δ and check the value of the chaos exponent $\alpha = 1$ as expected from droplet scaling?

Here will use the minimum cost flow algorithm described above to compute the two ground states h_i^1 and h_i^2 with free boundary conditions. Instead of computing the correlation function $C_{12}(r)$, we compute numerically the Fourier transform $S_{12}(q)$ of the 'overlap' between the configurations (17). Our simulations have been performed on a square lattice of linear size $L = 256$ and we have chosen $\mathbf{q} = (q, 0)$ with $q = 2\pi n/L$ with $n = 0, 1, 2, \ldots, L-1$. The disorder average has been performed over 10^6 independent

J. Stat. Mech. (2009) P08022

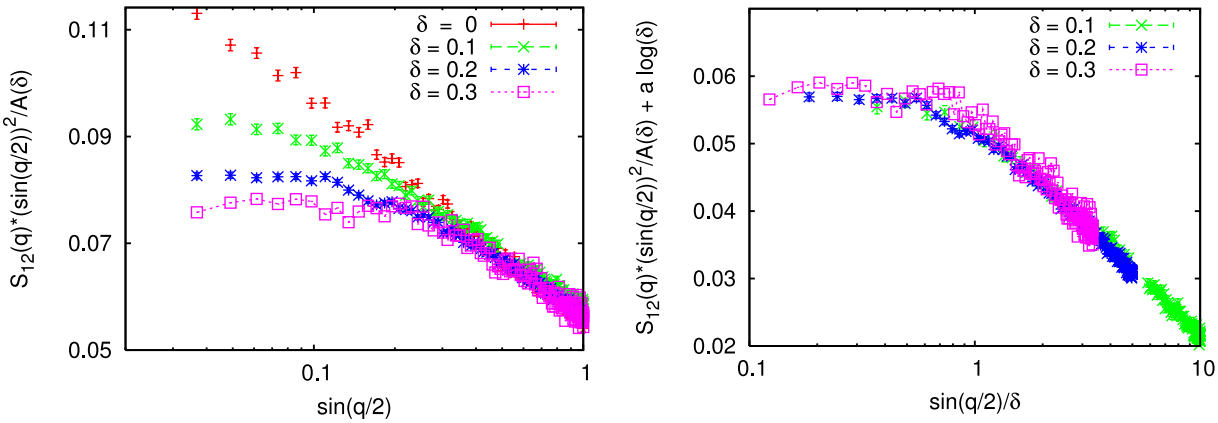

Figure 11. Left: plot of $S_{12}(q)y^2/A(\delta)$ as a function of $y = \sin(q/2)$ for different values of $\delta = 0, 0.1, 0.2, 0.3$ for a linear system size $L = 256$ on a log-linear scale. The deviation from the straight line for $\delta > 0$ is a clear indication of disorder chaos. This behavior is consistent with the one in equation (24) and in particular with a finite value of $\hat{\sigma}$ at $T = 0$. Right: same data as in the right panel, where we plot $y^2 S_{12}(q)/A(\delta) + a \log \delta$ as a function of y/δ. The relatively good collapse is consistent with the scaling form proposed in equation (26), implying in particular $\alpha = 1$.

samples. In figure 11 (left) we show our numerical data for $S_{12}(q)$. The behavior close to T_g, (24), suggests strongly plotting $q^2 S_{12}(q)$ as a function of q. Given that we are working on a discrete lattice of finite size, it is more convenient to work with the variable $y = \sin(q/2) = [(1 - \cos(q))/2]^{1/2}$ instead of q (of course for small q it makes no difference). In figure 11 (left) we actually show a plot of $S_{12}(q)[\sin(q/2)]^2/A(\delta)$ as a function of $\sin(q/2)$ on a log-linear plot for different values of $\delta = 0, 0.1, 0.2, 0.3$. On this plot the amplitude $A(\delta)$ is chosen such that the curves for different values of δ coincide for $\sin(q/2) \sim 1$, with $A(0) = 1$. For $\delta = 0$, where $S_{12}(q) = S_{11}(q)$, this plot is almost a straight line, which suggests that for small q where $\sin(q/2) \sim q/2$, it is indeed the case that $S_{11}(q) \sim \log(1/q)/q^2$: this produces the $\log^2(r)$ behavior of the correlation function $C_{11}(r)$ in real space. This result is consistent with previous numerical studies of the ground state[6].

For $\delta > 0$ the behavior is however quite different: indeed for small q, the curves deviate from the straight line indicating a saturation to a finite value. We have checked that this is not a finite size effect: in particular, for a given value of δ, we have checked that the value of q where the bending occurs and the saturating value do not depend on L. This bending is thus a clear signature of disorder chaos in this model. In addition, the saturation to a finite value is consistent with a positive value of $\hat{\sigma}$ at $T = 0$. If one translates these results into real space, one obtains a behavior of the correlation function $C_{12}(r) \propto \hat{\sigma} \log r$ as in equation (25). Of course $A(\delta) \to 1$ when $\delta \to 0$ but we were not able to characterize the dependence of $A(\delta)$ precisely. We emphasize that the observation

[6] In addition, this gives an alternative way to estimate the amplitude of the $\log^2(r)$ term; here $a_2 = 0.40$, which is slightly different from the previous estimate obtained from the fit of $C_{11}(r)$ in real space and yields $a_2 = 0.57$ (which is actually recovered in the present simulations by applying the same fitting procedure).

J. Stat. Mech. (2009) P08022

of disorder chaos here needs a precise computation of $q^2 S_{12}(q)$ and thus needs accurate statistics.

The scaling form in equation (19) would suggest plotting $q^2 S_{12}(q)$ as a function of $L^{2\zeta}\tilde{\varphi}(qL_\delta)$. Here one has $\zeta = 0$ together with $\alpha = 1$ expected from a scaling argument and, on the other hand, one expects (see figure 11 (left) and also equation (24)) to have $\tilde{\varphi}(x) \sim -a \log(x)$ for large x (with $a = 0.016(1)$ estimated from $q^2 S_{11}(q)$). Therefore, to guarantee that $S_{12}(q)$ has a good limit when $\delta \to 0$, we propose the scaling form

$$S_{12}(q) \sim q^{-2}\left(\tilde{\varphi}\left(\frac{q}{\delta}\right) - a \log \delta\right), \tag{26}$$

where the scaling function $\tilde{\varphi}(z)$ behaves like

$$\tilde{\varphi}(z) = \begin{cases} c^{\mathrm{st}}, & z \to 0, \\ -a \log z, & z \to \infty, \end{cases} \tag{27}$$

such that the additional constant $-a \log \delta$ with $a = 0.016(1)$ (independently of δ) is needed to yield a well defined limit $\delta \to 0$. We have checked this scaling form (26) for different values of $\delta = 0.1, 0.2, 0.3$. Again, to take into account finite size effects, we use the variable $y = \sin(q/2)$ instead of q. In figure 11 (right) we show a plot of $y^2 S_{12}(q)/A(\delta) + a \log \delta$ as a function of y/δ. The relatively good collapse of these curves corresponding to different values of δ is in rather good agreement with the scaling in equation (26). This indicates in particular that $\alpha \simeq 1$, although a study of $S_{12}(q)$ for smaller values of δ would certainly be necessary for obtaining a more precise estimate of this exponent.

5. Discussion

We found that the left passage probability of zero-temperature domain walls in the disordered SOS model in different geometries agrees well (within the numerical error bars) with Schramm's formula for $\kappa = 4$. Since the fractal dimension of the domain walls is $d_{\mathrm{s}} = 1.25 \pm 0.01$ this is inconsistent with $d_{\mathrm{s}} = 1 + \kappa/8 = 1.5$ which should hold if this ensemble of random curves could be described as showing SLE. One condition for SLE to hold is that the measure of the ensemble of random curves obeys a domain Markov property. Checking this numerically is a computationally extremely challenging endeavor (cf [24]) and we did not attempt it here. The second condition for SLE is that the measure is invariant under a conformal mapping of the domain within which the random curves are defined. In our study we considered several different domain shapes and we found that in all cases the left passage probability is represented by Schramm's formula adapted via a conformal map to the specific geometry under consideration. Although not being a sufficient criterion for conformal invariance to hold in general, this observation is at least surprising as regards the fact that κ and d_{s} do not obey the SLE prediction. To shed light on this issue, further tests of conformal invariance are worthwhile.

Interestingly the contour loops in this system (i.e. the lines connecting sites of equal height in the ground state) have a fractal dimension close to $d_{\mathrm{f}} = 1.5$ [39], the same dimension as the contour loops in the SOS model *without* disorder at finite temperatures above the critical temperature [22, 40]. The latter *can* indeed be described as showing SLE with $\kappa = 4$ [22, 40]. It remains to be checked whether the contour loops in the disordered SOS model can also be described as showing SLE with $\kappa = 4$.

J. Stat. Mech. (2009) P08022

The boundaries of droplets, i.e. connected clusters of a given lateral size that have a minimal excitation energy, have the same fractal dimension as domain walls ($d_s = 1.25$), but their energy ΔE_l saturates at a small, finite value for increasing lateral size l. In [20] it was shown that the mean droplet energy ΔE_L decreases with system size L like $\Delta E_L^{-1} \sim \ln L$. This result is actually consistent with ours, since in [20] the droplet size was only restricted by an upper bound (the system size L) but not by a lower bound as in our study. So the result for ΔE_L is the optimal excitation among typically $\log L$ excitations of fixed (maximum and minimum) size l. *If* the distribution of the energies of these excitations on different length scales is independent of the length scale, *then* ΔE_L is just the minimum of $\ln L$ independent, identically distributed random numbers, and thus proportional to $1/\ln L$. What we show in our study is essentially that this assumption is indeed fulfilled, as shown in figure 10. This is a non-trivial result and does not immediately follow from a vanishing stiffness exponent, $\theta = 0$. With a view towards their entropic contribution one would like to know how the number of independent (i.e. spatially disjoint) droplets scales with their size. It should be possible to study these challenging questions with the methods that we presented.

Finally, we have shown that there is disorder chaos at $T = 0$ in this model. Our numerical data show a behavior of interlayer correlations $S_{12}(q)$ compatible with equation (24) with $\hat{\sigma} > 0$, and thus rather similar to the one obtained close to T_g [44]. Here, the two ground states of the system, embedded in two slightly different disorder realizations, thus display logarithmic residual correlations. In addition, our data are consistent with a chaos exponent $\alpha = 1$, in agreement with the droplet scaling argument. Following the studies of [34, 43, 45] it would certainly be interesting to describe these behaviors analytically by means of a detailed analysis of the model in equation (23) at $T = 0$. Of course, and especially in view of recent analytical progress [45], it would also be very interesting to extend these studies of disorder chaos to finite temperature, which we expect to play a role here in this marginal glass phase.

Acknowledgment

We would like to thank P Le Doussal for useful discussions.

References

[1] Bray A J and Moore M A, *Chaotic nature of the spin glass phase*, 1987 *Phys. Rev. Lett.* **58** 57
[2] Fisher D S and Huse D A, *Equilibrium behavior of the spin glass ordered phase*, 1988 *Phys. Rev.* B **38** 386
Fisher D S and Huse D A, *Non-equilibrium dynamics of spin glasses*, 1988 *Phys. Rev.* B **38** 373
[3] Rieger H, Santen L, Blasum U, Diehl M, Jünger M and Rinaldi G, *The critical exponents of the two-dimensional Ising spin glass revisited—exact ground state calculations and Monte Carlo simulations*, 1996 *J. Phys. A: Math. Gen.* **29** 3939
Kawashima N and Rieger H, *Finite size scaling analysis of exact ground states for ± spin glass models in two dimensions*, 1997 *Europhys. Lett.* **39** 85
[4] Kawashima N, *Fractal droplets in two dimensional spin glasses*, 2000 *J. Phys. Soc. J.* **69** 987
[5] Hartmann A K and Young A P, *Lower critical dimension of Ising spin glasses*, 2001 *Phys. Rev.* B **64** 180404
[6] Amoruso C, Marinari E, Martin O C and Pagnani A, *Scalings of domain wall energies in two dimensional Ising spin glasses*, 2003 *Phys. Rev. Lett.* **91** 087201
[7] Sasaki M, Hukushima K, Yoshino H and Takayama H, *Temperature chaos and bond chaos in the Edwards–Anderson Ising spin glass—domain wall free energy measurements*, 2005 *Phys. Rev. Lett.* **95** 267203
[8] Hartmann A K, *Droplets in the two-dimensional ±J spin glass*, 2008 *Phys. Rev.* B **77** 144418

J. Stat. Mech. (2009) P08022

[9] Weigel M and Gingras M J P, *Ground states and defect energies of the two-dimensional XY spin glass from a quasi-exact algorithm*, 2006 *Phys. Rev. Lett.* **96** 097206
Weigel M and Gingras M J P, *Zero-temperature phase of the XY spin glass in two dimensions*, 2008 *Phys. Rev.* B **77** 104437
[10] Nattermann T, Shapir Y and Vilfan I, *Interface pinning and dynamics in random systems*, 1990 *Phys. Rev.* B **42** 8577
[11] Nattermann T, *Theory of the random field Ising model*, 1997 *Spin Glasses and Random Fields* ed A P Young (Singapore: World Scientific)
[12] Seppälä E T, Petäjä V and Alava M J, *Disorder, order, and domain wall roughening in the 2d random field Ising model*, 1998 *Phys. Rev.* E **58** R5217
Alava M and Rieger H, *Chaos in the random field Ising model*, 1998 *Phys. Rev.* E **58** 4284
[13] Middleton A A and Fisher D S, *The three-dimensional random field Ising magnet: interfaces, scaling, and the nature of states*, 2002 *Phys. Rev.* B **65** 134411
[14] Fisher D S and Huse D, *Directed paths in a random potential*, 1991 *Phys. Rev.* B **43** 10728
[15] Fisher D S, *Stability of elastic glass phases in random field XY magnets and vortex lattices*, 1997 *Phys. Rev. Lett.* **78** 1964
[16] Rieger H and Blasum U, *Ground state properties of solid-on-solid models with disordered substrates*, 1997 *Phys. Rev.* B **55** R11981
[17] Middleton A A, *Numerical investigation of the thermodynamic limit for ground states in models with quenched disorder*, 1999 *Phys. Rev. Lett.* **83** 1672
[18] Pfeiffer F and Rieger H, *Dislocations in the ground state of the solid-on-solid model on a disordered substrate*, 2000 *J. Phys. A: Math. Gen.* **33** 2489
[19] Middleton A A, *Disorder-induced topological defects in a $d = 2$ elastic medium at zero temperature*, 2000 *Phys. Rev.* B **61** 14787
[20] Middleton A A, *Energetics and geometry of excitations in random systems*, 2001 *Phys. Rev.* B **63** 060202
[21] Bauer M and Bernard D, *2D growth processes: SLE and Loewner chains*, 2006 *Phys. Rep.* **432** 115
[22] Cardy J, *SLE for theoretical physicists*, 2005 *Ann. Phys., NY* **318** 81
[23] Amoruso C, Hartmann A K, Hastings M B and Moore M A, *Conformal invariance and stochastic Loewner evolution process in two-dimensional Ising spin glasses*, 2006 *Phys. Rev. Lett.* **97** 267202
[24] Bernard D, Le Doussal P and Middleton A A, *Possible description of domain walls in two-dimensional spin glasses by stochastic Loewner evolutions*, 2007 *Phys. Rev.* B **76** 020403(R)
[25] Risau-Gusman S and Romá F, *Fractal dimension of domain walls in the Edwards–Anderson spin glass model*, 2008 *Phys. Rev.* B **77** 13445
[26] Jacobsen J L, Le Doussal P, Picco M, Santachiara R and Wiese K J, *Critical Interfaces in the random-bond Potts model*, 2009 *Phys. Rev. Lett.* **102** 070601
[27] Giamarchi T and Le Doussal P, *Elastic theory of flux lattices in presence of weak disorder*, 1995 *Phys. Rev.* B **52** 1242
[28] Nattermann T and Scheidl S, *Vortex-glass phases in type-II superconductors*, 2000 *Adv. Phys.* **49** 607
[29] For an exhaustive list of references see: Carpentier D and Le Doussal P, *Glass phase of two-dimensional triangular elastic lattices with disorder*, 1997 *Phys. Rev.* B **55** 12128
[30] Cardy J L and Ostlund S, *Random symmetry-breaking fields and the XY model*, 1982 *Phys. Rev.* B **25** 6899
[31] Zeng C, Leath P L and Hwa T, *Thermodynamics of Mesoscopic Vortex Systems in 1+1 Dimensions*, 1999 *Phys. Rev. Lett.* **83** 4860
[32] Zeng C, Middleton A A and Shapir Y, *Ground-state roughness of the disordered substrate and flux lines in $d = 2$*, 1996 *Phys. Rev. Lett.* **77** 3204
[33] Guruswamy S, LeClair A and Ludwig A W W, *$gl(N|N)$ super-current algebra for disordered Dirac fermions in two dimensions*, 2000 *Nucl. Phys.* B **583** 475
[34] Le Doussal P and Schehr G, *Disordered free fermions and the Cardy Ostlund fixed line at low temperature*, 2007 *Phys. Rev.* B **75** 184401
[35] Schulz U, Villain J, Brézin E and Orland H, *Thermal fluctuations in some random field models*, 1988 *J. Stat. Phys.* **51** 1
[36] Blasum U, Hochstätter W, Moll C and Rieger H, *Using network-flow techniques to solve an optimization problem from surface-physics*, 1996 *J. Phys. A: Math. Gen.* **29** L459
Rieger H, *Ground state properties of flux-lines in disordered environments*, 1998 *Phys. Rev. Lett.* **81** 4488
[37] Hartmann A K and Rieger H, 2001 *Optimization Algorithms in Physics* (Berlin: Wiley–VCH)
[38] Schramm O, *A percolation formula*, 2001 *Electron. Commun. Probab.* **6** 115
[39] Zeng C, Kondev J, McNamara D and Middleton A A, *Statistical topography of glassy interfaces*, 1998 *Phys. Rev. Lett.* **80** 109

J. Stat. Mech. (2009) P08022

[40] Schramm O and Sheffield S, *Contour lines of the two-dimensional discrete free field*, 2009 *Acta Math.* **202** 21
[41] Krzakala F and Bouchaud J-P, *Disorder chaos in spin glasses*, 2005 *Europhys. Lett.* **72** 472
[42] Shapir Y, *Response of manifolds pinned by quenched impurities to uniform and random perturbations*, 1991 *Phys. Rev. Lett.* **66** 1473
[43] Le Doussal P, *Chaos and residual correlations in pinned disordered systems*, 2006 *Phys. Rev. Lett.* **96** 235702
[44] Hwa T and Fisher D S, *Vortex glass phase and universal susceptibility variations in planar arrays of flux lines*, 1994 *Phys. Rev. Lett.* **72** 2466
[45] Duemmer O and Le Doussal P, *Chaos in the thermal regime for pinned manifolds via functional RG*, 2007 arXiv:0709.1378v1
[46] Schehr G and Le Doussal P, *Exact multilocal renormalization on the effective action: application to the random sine Gordon model statics and non-equilibrium dynamics*, 2003 *Phys. Rev.* E **68** 046101

J. Stat. Mech. (2009) P08022